Pharm Res (2013) 30:280–289
DOI 10.1007/s11095-012-0872-8

RESEARCH PAPER

Exploring the Solid-Form Landscape of Pharmaceutical Hydrates: Transformation Pathways of the Sodium Naproxen Anhydrate-Hydrate System

Dhara Raijada • Andrew D. Bond • Flemming H. Larsen • Claus Cornett • Haiyan Qu • Jukka Rantanen

Received: 18 June 2012 / Accepted: 20 August 2012 / Published online: 21 September 2012

ABSTRACT

Purpose To understand the transformation pathways amongst anhydrate/hydrate solid forms of sodium naproxen and to highlight the importance of a polymorphic dihydrate within this context.

Methods Multi-temperature dynamic vapour sorption (DVS) analysis combined with variable-humidity X-ray powder diffraction (XRPD) to establish the transformation pathways as a function of temperature and humidity. XRPD and thermogravimetric analysis (TGA) to characterise bulk samples. Monitoring of *in-situ* dehydration using solid-state ^{13}C CP/MAS spectroscopy.

Results At 25°C, anhydrous sodium naproxen (AH) transforms directly to one dihydrate polymorph (DH-II). At 50°C, AH transforms stepwise to a monohydrate (MH) then to the other dihydrate polymorph (DH-I). DH-II transforms to a tetrahydrate (TH) more readily than DH-I transforms to TH. Both dihydrate polymorphs transform to the same MH.

Conclusions The properties of the polymorphic dihydrate control the transformation pathways of sodium naproxen.

KEY WORDS dynamic vapour sorption · hydrates · sodium naproxen · solid-state NMR spectroscopy

INTRODUCTION

There is a practical need to monitor and control the hydration state of active pharmaceutical compounds as a function of temperature and relative humidity in order to ensure constant quality for drug products. To this end, measurement of hygroscopicity by dynamic vapour sorption (DVS) analysis is a routine practice during pharmaceutical preformulation studies. For compounds that can exist in various anhydrate/hydrate solid forms, DVS data can provide a convenient overview of the transformations that occur between forms. Early identification and investigation of any such transformations is crucial during product development because transformations amongst anhydrate/hydrate forms can have a significant impact on product performance (1–5). In seeking to understand the nature of any observed transformations, it is important to add structural and thermodynamic information to the empirical DVS data. One complication that can arise during such an exercise is the possibility of polymorphism for any of the anhydrate/hydrate forms (4,6). Under such circumstances, polymorphic solid forms with the same hydration state might exhibit different degrees of stability or different transformation

Electronic supplementary material The online version of this article (doi:10.1007/s11095-012-0872-8) contains supplementary material, which is available to authorized users.

D. Raijada · C. Cornett · J. Rantanen (✉)
Department of Pharmacy, Faculty of Health and Medical Sciences
University of Copenhagen
Universitetsparken 2
Copenhagen 2100, Denmark
e-mail: jukka.rantanen@sund.ku.dk

A. D. Bond
Department of Physics, Chemistry and Pharmacy
University of Southern Denmark
Odense 5230, Denmark

F. H. Larsen
Department of Food Science, Faculty of Life Sciences
University of Copenhagen
Frederiksberg C 1958, Denmark

H. Qu
Institute of Chemical Engineering, Biotechnology and Environmental Technology
University of Southern Denmark
Odense 5230, Denmark

pathways (7–9). Therefore, pharmaceutical hydrates have been a widespread topic of discussion, both in the pharmaceutical field (10–16), and also in the crystal engineering literature (15,17,18). In the latter, reports of polymorphic hydrates are becoming increasingly frequent, and there are also indications that water molecules might be applied as specific design elements within molecular crystals.

In this paper, we consider one model compound with an established set of anhydrate/hydrate forms, where the dihydrate is known to be polymorphic. Our interest in particular is to investigate the influence of the dihydrate polymorphism on the transformation pathways. The selected compound is sodium (*S*)-naproxen (Fig. 1), which is a non-steroidal anti-inflammatory drug (NSAID). Sodium naproxen is known to exist as an anhydrate (AH), a monohydrate (MH), two dihydrate polymorphs (DH-I and DH-II), and a tetrahydrate (TH) (19–22). A study of the thermodynamic and kinetic aspects of the system has been reported recently by Malaj *et al.* (21). Those authors refer to the various phases as ASN (= AH), MSN (= MH), CSN (= DH-I), DSN (= DH-II) and TSN (= TH). We have studied sodium naproxen using a multi-temperature DVS protocol, combined with variable-temperature/variable-humidity X-ray powder diffraction (XRPD), and it is shown here that this approach can provide a rich source of information to characterise the transformation pathways in this complex case. Consideration of the DVS and XRPD data as a function of temperature and humidity also provides a convenient means to identify optimal static conditions to generate bulk samples of the various forms. The significant influence of the polymorphic dihydrate on the observed transformation pathways is discussed. We note that other hyphenated techniques, such as DVS combined with Raman or NIR spectroscopy, might also be used in this context (23–26). In the case of sodium naproxen, however, we have found that these spectroscopic techniques can not reliably distinguish the various anhydrate/hydrate forms.

MATERIALS AND METHODS

Materials

Sodium (*S*)-naproxen anhydrate (AH) (USP grade) was received from Divi's Laboratories Limited, India. Saturated salt solutions of magnesium nitrate hexahydrate and potassium sulphate (both from VWR International, Leuven, Belgium) were used respectively to create static 55% RH and 95% RH conditions at 25°C. Sodium bromide (Merck KGaA, Darmstadt, Germany) and potassium chloride (J.T. Baker, Deventer, Holland) were used respectively for generation of static 50% RH and 80% RH conditions at 50°C. Bulk samples of MH and DH-I were generated by exposing AH to 50°C/50% RH and 50°C/80% RH, respectively. Bulk samples of DH-II and TH were generated by exposing AH to 25°C/55% RH and 25°C/95% RH, respectively, as discussed in the Results section.

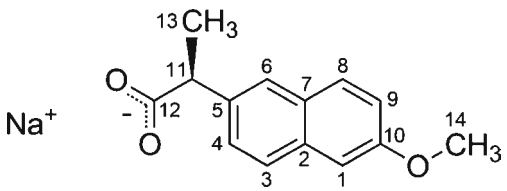

Fig. 1 Chemical structure of sodium (*S*)-naproxen.

Methods

Dynamic Vapour Sorption (DVS)

DVS analysis was performed using a Symmetrical Gravimetric Analyzer (SGA-100) (VTI Corp., Hialeah, FL). Around 8 mg of AH was used as the starting material. The humidity was varied with a ramping step of 5% RH in two cycles of sorption–desorption: 10% RH→95% RH (sorption 1), 95% RH→10% RH (desorption 1), 10% RH→95% RH (sorption 2), and 95% RH→10% RH (desorption 2). The equilibration criterion was taken to be 0.01% *w/w* or a maximum step time of 180 min. The measurements were performed at temperatures of 25, 30, 35, 40, 45 and 50°C. The raw data for the first sorption cycle at each temperature and humidity were imported to SigmaPlot 11.0 (Systat Software, Inc., San Jose, CA) for construction of the 3-dimensional empirically-derived phase diagram.

X-ray Powder Diffraction (XRPD)

X-Ray powder diffraction (XRPD) patterns were recorded at room temperature in Bragg-Brentano geometry using a PANalytical X'Pert Pro diffractometer equipped with a PIXcel detector (PANalytical B.V., Almelo, The Netherlands). The radiation was non-monochromated CuKα (λ=1.5418 Å). A continuous 2θ scan was performed in the range 2-40° with a point resolution of 0.026° and a total measurement time of *ca* 10 mins. This corresponds to 96.4 s per data point using the 256-pixel detector. Variable temperature, variable humidity and vacuum measurements were carried out on the same system using an Anton Parr CHC-Plus chamber (Anton Parr GmbH, Graz, Austria) equipped with an MHG humidity generator (PMT Analytical GmbH, Ulm, Germany). Height alignment of the stage was calibrated prior to each run by measurement of a standard AH pattern. Samples were held at a fixed temperature of either 25 or 50°C and the RH was ramped upwards in steps of 10% RH. At each RH step, XRPD patterns were measured repeatedly using the conditions described above until no further change was observed in the pattern. *In situ* dehydration experiments were performed

on the same sample stage (i) at 25 or −5°C for MH and DH, respectively, by creating a vacuum of around 0.01 millibar; (ii) at 25 and 40°C for DH under ambient conditions. Data were collected using X'Pert Data Collector version 2.2 and analyzed with X'Pert Highscore Plus version 2.2.4 (PANalytical B.V., Almelo, The Netherlands).

Thermogravimetric Analysis (TGA)

TGA thermograms were measured using a TGA 7 instrument (Perkin Elmer, Norwich, CT). The temperature was calibrated using a ferromagnetic standard and weight calibration was performed using a 100 mg standard. Samples (4–5 mg) of the sodium naproxen solid forms were analyzed in a flame-cleansed Pt pan under open conditions at a heating rate of 10°C/min with a dry nitrogen purge of 20 ml/min.

Solid-State NMR Spectroscopy

The NMR spectra were recorded on a Bruker Avance 400 spectrometer (Bruker Biospin, GmbH, Karlsruhe, Germany) operating at Larmor frequencies of 100.62 and 400.13 MHz for ^{13}C and ^{1}H, respectively, using a double-tuned CP/MAS (Cross polarization/Magic Angle Spinning) probe equipped for 4 mm (o.d.) rotors. The ^{13}C CP/MAS spectra were recorded using a contact time of 8.5 ms, a spin-rate of 12 kHz, a recycle delay of 8 s, an acquisition time of 40.9 ms during which ^{1}H TPPM decoupling (80 kHz rf-field strength) was employed (27), and 256 scans. The cross polarization was carried out using variable amplitude CP (28) with a maximum rf-field strength of 80 kHz for both ^{1}H and ^{13}C. ^{13}C chemical shifts were referenced to an external sample of α-glycine (carbonyl group) at 176.5 ppm. Time series ^{13}C CP/MAS spectra of DH-I and DH-II were performed at temperatures of 40°C, 50°C and 60°C. The temperature was controlled using a Bruker temperature controller. Due to the frictional heating induced by spinning, the exact temperature was determined from ^{1}H spectra of an external sample of ethylene glycol at the actual temperature setting and spin rate. Data were processed using TopSpin 2.1 (Bruker Biospin GmbH, Karlsruhe, Germany) and then transferred to Matlab 7.11.0 (MathWorks Inc., Natick, MA) to set up figures.

RESULTS

Dynamic Vapour Sorption (DVS)

An outline of the hydration and dehydration pathways for the sodium naproxen system is shown by dynamic vapour sorption (DVS) analysis, whereby the mass uptake of the solid compound is monitored as a function of relative humidity (Fig. 2). To assess the influence of temperature, the DVS analyses were repeated at 5°C intervals in the range of 25 to 50°C, in each case using AH as the starting compound (Fig. 2 and Supplementary Fig. S1). At 25°C, AH transforms directly to DH (*i.e.* without any detectable intermediate plateau at the step size of 5% RH; the polymorphic phase of DH is unspecified during the DVS analysis) above a critical relative humidity (RH) of ~50% (Fig. 2a). With increasing humidity, DH remains stable until ~70% RH before transformation takes place to TH. Hysteresis is observed in the dehydration cycle, whereby TH transforms back to DH below ~50% RH, then DH transforms gradually to MH below ~30% RH. Further dehydration to regenerate AH is not seen down to the lower measured limit of ~10% RH. Dehydration of MH to AH at 0% RH has been shown previously (20) to be slow (taking up to months), so we would not expect to observe this process during the DVS trials. In the second sorption cycle, MH transforms to DH at ~55% RH, then transformation of DH to TH takes place at ~85% RH. Subsequent desorption/sorption cycles then follow the same loop. Different behaviour is observed as the temperature is increased. At the highest examined temperature of 50°C, AH transforms to MH at ~50% RH, then MH transforms to DH at ~70% RH (Fig. 2b). TH is not seen at this temperature. Dehydration of DH to MH occurs relatively abruptly with moderate hysteresis, then subsequent sorption/desorption cycles are identical to the first cycles.

Variable-Humidity X-Ray Powder Diffraction (VH-XRPD)

The DVS results were correlated with structural changes using variable-humidity X-ray powder diffraction (VH-XRPD). The results for the sorption processes at 25 and 50°C are shown in Fig. 3. Each XRPD pattern could be matched clearly to those established for the various bulk phases (as shown in Fig. 5), including identification of DH-II and DH-I as polymorphic dihydrates in the first sorption cycles at 25°C and 50°C, respectively. At 25°C, XRPD confirms that AH transforms directly to DH-II, without any detectable MH intermediate. Moreover, AH was stable under static condition of 50% RH at 25°C, while direct transformation from AH to DH-II was observed under static condition of 55% RH at 25°C (Supplementary Fig. S2). This also illustrates that MH cannot be generated directly from AH at 25°C. At 50°C, conversion of AH to MH is identified at 50% RH, followed by transformation to DH-I at 70% RH. Separate analyses starting from a bulk sample of MH confirmed that MH also transforms to DH-I at 25°C/60% RH, as seen in the second DVS sorption cycle. Allowing TH to dehydrate within the XRPD chamber at 25°C generated a mixture of DH-I and DH-II. Thus, the structural details of the DVS analyses are as follows: at 25°C, the first sorption cycle follows the sequence AH→DH-II→

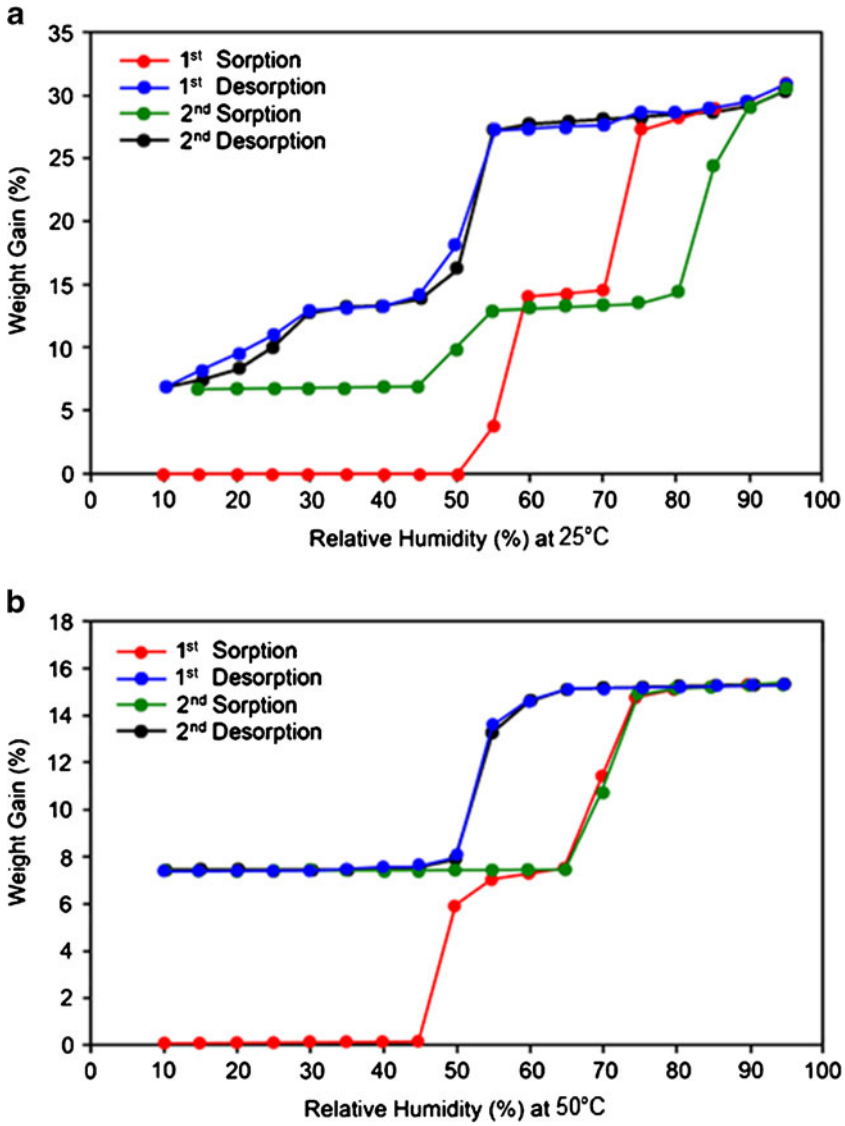

Fig. 2 Dynamic vapour sorption (DVS) traces at (**a**) 25°C and (**b**) 50°C. (Theoretical water content: MH (6.7%), DH (12.5%), TH (22.2%)).

TH, all desorption cycles follow TH→DH-I/DH-II→MH, and the second and subsequent sorption cycles follow MH→DH-I→TH. At 50°C, the first sorption cycle follows the sequence AH→MH→DH-I, then the system enters into a consistent desorption/sorption cycle involving MH and DH-I.

Identifying Optimal Static Conditions for Generation of the Solid Forms

Three-dimensional plotting of the multi-temperature DVS data sets provides a graphical representation of the measured weight gain as a function of both temperature and humidity. This can be considered to provide an empirically-derived phase diagram showing the regions of existence for the various solid forms. Figure 4 depicts the data for the first sorption cycles at different temperatures, thereby showing the regions of stability for generation of various solid forms. It can be seen immediately from the diagram that MH can only be formed from AH at temperatures above *ca* 40°C, and TH can exist only below *ca* 45°C. The plateaux in the plot identify the stable regions where various solid forms can be isolated. Accordingly, bulk samples of MH, DH-I, DH-II and TH were generated by exposing AH in desiccators for around 1 week at 50°C/50% RH, 50°C/80% RH, 25°C/55% RH and 25°C/95% RH, respectively. It should be noted that the diagram in Fig. 4 refers specifically to transformations in the direction of increasing humidity starting from AH. The DVS analyses show that the system is not directly reversible during desorption, so the diagram should not be viewed as a proper thermodynamic phase diagram.

Characterization of the Bulk Samples

Morphological characterization of the bulk samples by scanning electron microscopy is described in the Supplementary Material.

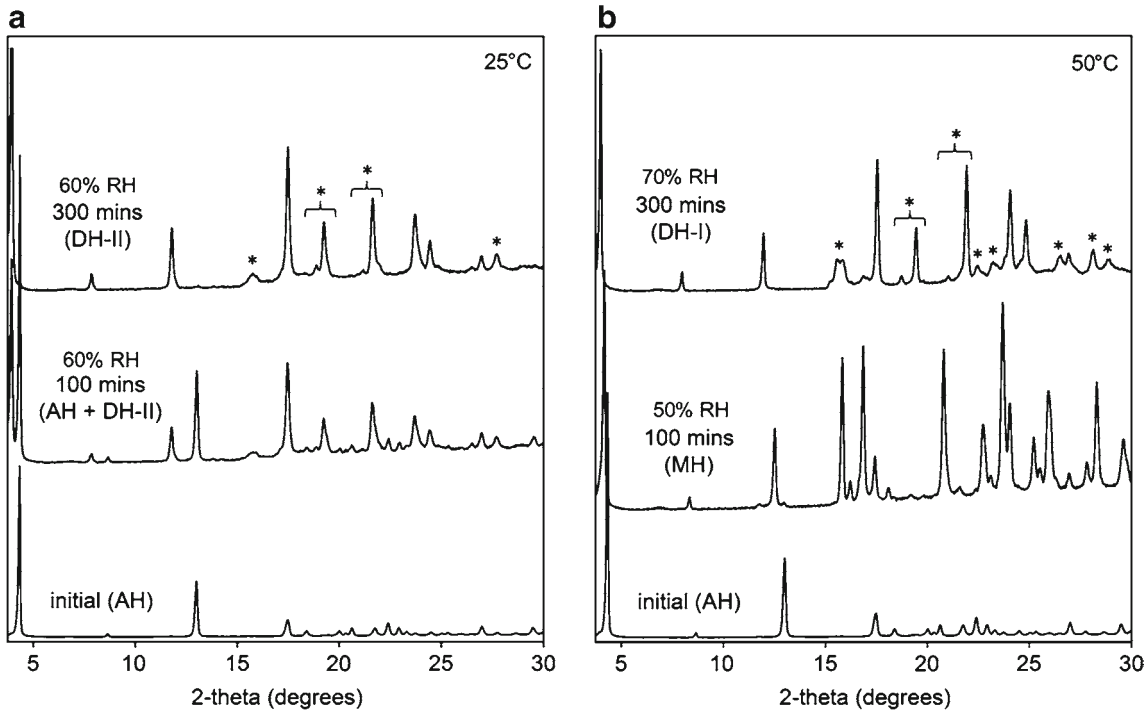

Fig. 3 Variable-humidity XRPD results at (**a**) 25°C and (**b**) 50°C. (* denotes characteristic differences in the patterns of DH-I and DH-II).

X-Ray Powder Diffraction

XRPD patterns of the bulk samples obtained under the specified static conditions confirm their structural identity (Fig. 5). These patterns are comparable to those reported by Malaj *et al.* (21) except that the structural purity appears to be slightly improved, particularly for MH. The XRPD patterns of DH-I and DH-II are sufficiently different to provide signature patterns for the two polymorphs. The principal diagnostic features that we consider are the slight shift to lower 2θ values for the first three peaks in the diffraction pattern for DH-II compared to DH-I, a smaller spacing between the pair of peaks at 2θ=18.9/19.3° and 21.2/21.7° (DH-II) compared to 18.8/19.5° and 21.0/22.0° (DH-I), and the distinct pairs of peaks at 34.5/38.2° (DH-II) compared to 35.1/38.9° (DH-I).

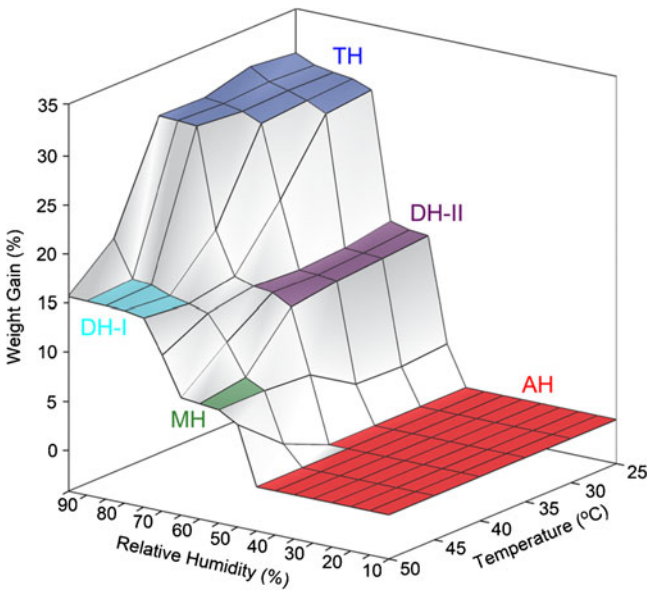

Fig. 4 A three-dimensional empirically-derived phase diagram based on DVS sorption data. (The resolution of the RH and temperature axes is 5% RH and 5°C, respectively.)

Thermogravimetric Analysis (TGA)

Weight loss for the bulk samples was found by thermogravimetric analysis (TGA) to be 6.6, 12.4, 12.5 and 22.5% for MH, DH-I, DH-II and TH, respectively. These values are in good agreement with the theoretical water contents of MH (6.7%), DH (12.5%) and TH (22.2%). Our TGA data (Fig. 6) are comparable to those reported by Malaj *et al.* (21), but the specific details of the traces are of interest in relation to the different dehydration behaviour observed for the dihydrate polymorphs. It can be seen from Fig. 6 that DH-I shows a pronounced plateau corresponding to MH, while DH-II shows a more smooth transition to AH. TH loses three water molecules in an apparently continuous manner before showing a plateau corresponding to MH, suggesting that water loss from TH during the TGA analysis is accompanied by simultaneous dehydration of any intermediate DH form.

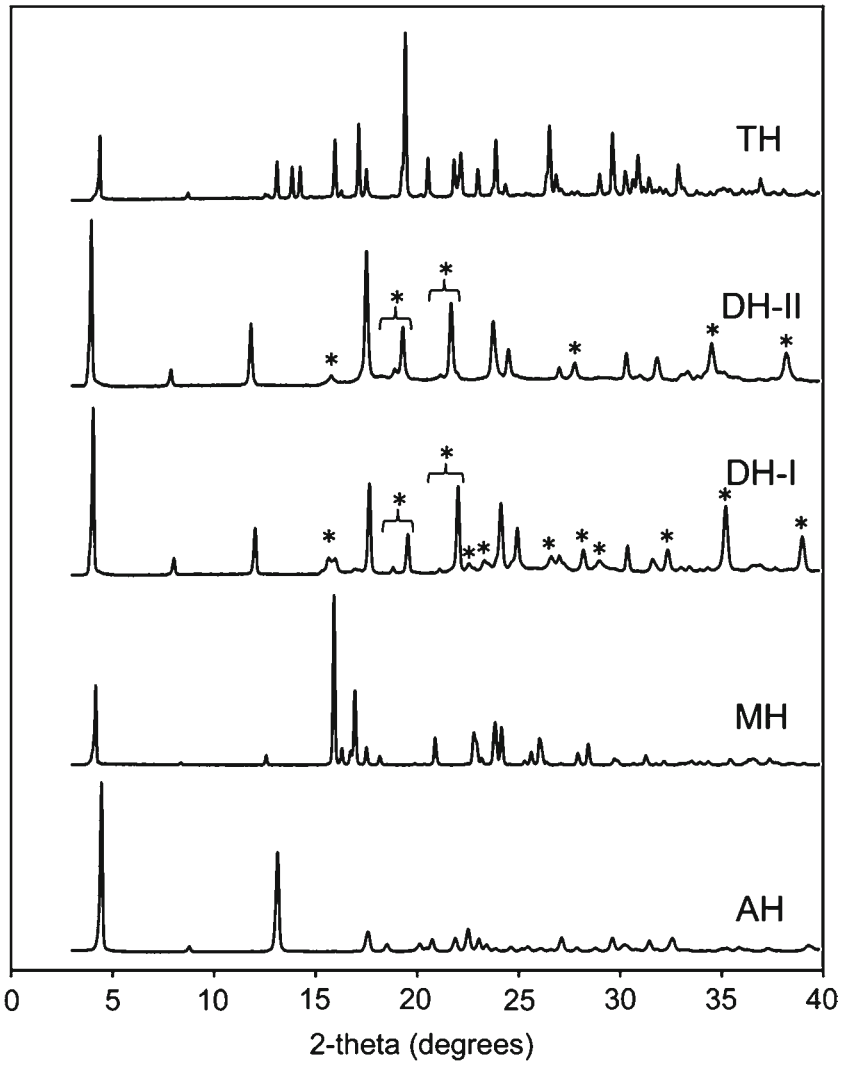

Fig. 5 Standard XRPD patterns for the sodium naproxen anhydrate/hydrate forms. (* denotes characteristic differences in the patterns of DH-I and DH-II).

Dehydration of DH-I and DH-II

The desorption cycles of the DVS illustrate dehydration of the dihydrate forms as the humidity is reduced at constant temperature. XRPD data under these conditions confirm that both DH-I and DH-II convert principally to MH. Alternatively, the TGA data show how DH-I and DH-II transform on heating. The difference in the shapes of the two TGA curves, in particular the more pronounced plateau corresponding to MH in the thermogram of DH-I, suggest different pathways for these transformations. *In situ* dehydration experiments were performed in XRPD under vacuum at −5°C and under ambient pressure at 25 and 40°C to explore the potential structural differences in the transformation pathways of the two dihydrates. The results for dehydration under vacuum at −5°C revealed direct transformation from DH-II to AH, while transformation of DH-I to AH takes place *via* intermediate MH. On the other hand, at 40°C under ambient pressure, both DH-I and DH-II transform mainly to MH. However, some residue of AH is generated simultaneously with MH upon dehydration of DH-II at ambient pressure.

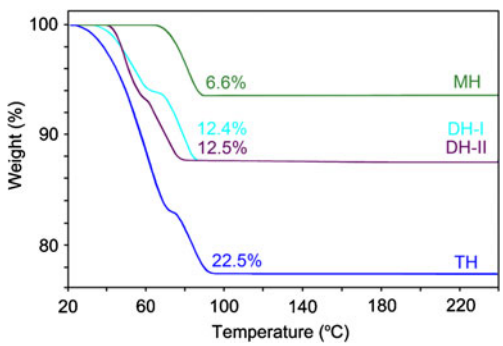

Fig. 6 TGA thermograms for MH, DH-I, DH-II and TH.

In situ thermal dehydration experiments were performed using solid-state ^{13}C CP/MAS NMR spectroscopy (Fig. 7) to obtain detailed structural information during dehydration. The peak assignment in the ^{13}C CP/MAS spectra is made according to previous reports (22,29). At 40°C, the

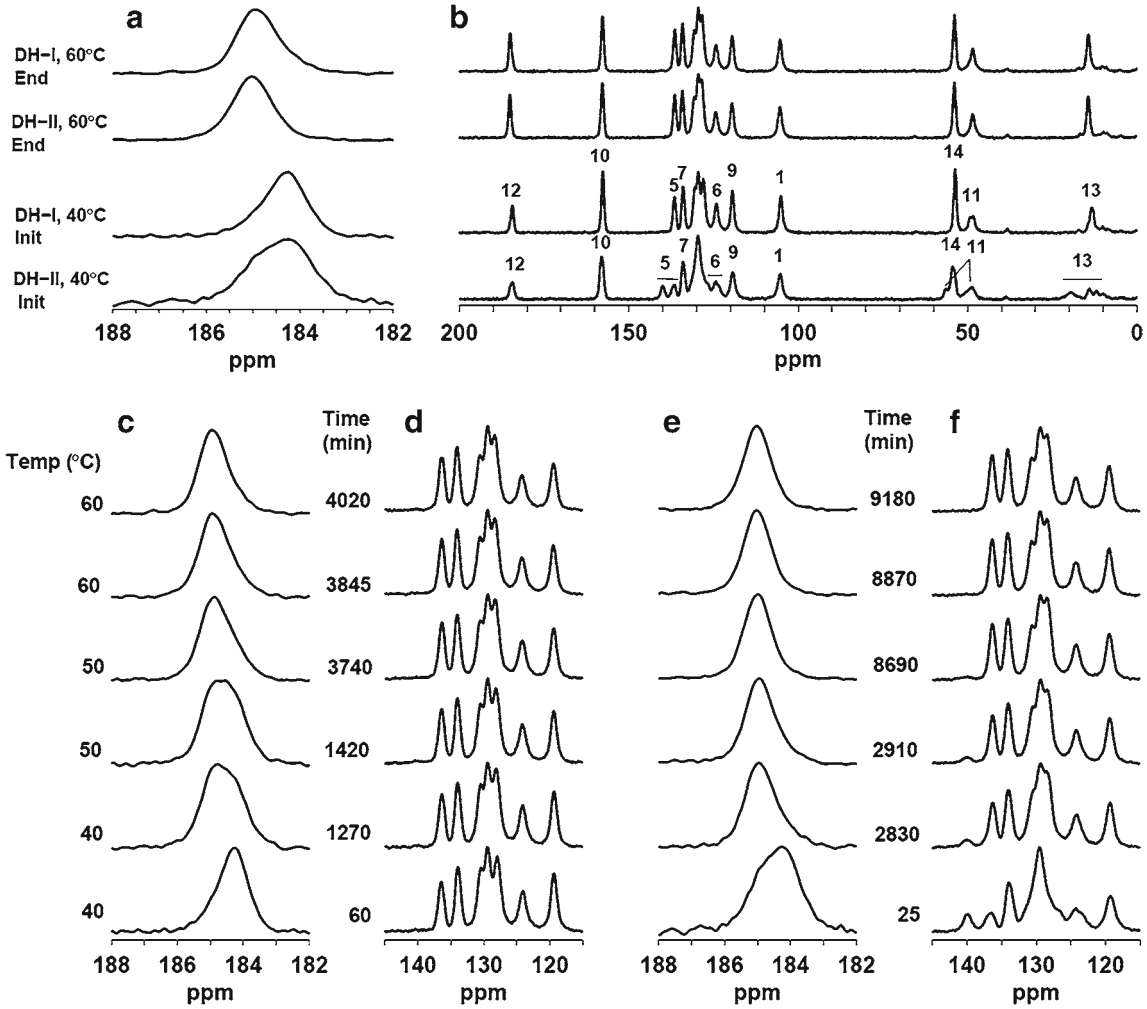

Fig. 7 Solid-state ^{13}C CP/MAS NMR spectra during *in-situ* dehydration of DH-I (**a**), (**b**), (**c**), (**d**) and DH-II (**a**), (**b**), (**e**), (**f**). The spectra in (**a**) and (**b**) display the initial and final spectra before and after *in-situ* dehydration, whereas the spectra in (**c**), (**d**), (**e**), (**f**) display spectra recorded during *in-situ* dehydration. (The atom numbering scheme corresponds to that in Fig. 1.).

initial ^{13}C CP/MAS NMR spectra for DH-I and DH-II (Fig. 7a and b) are clearly different. Broader lines are observed in the spectrum of DH-II compared to DH-I, suggesting some degree of disorder in DH-II. Furthermore, the sites C11 and C13 in DH-II situated in the propionate side chain close to sodium, are split into two resonances; likewise for sites C6 and C7 in the aromatic ring. In DH-I, only the peak of site C11 shows two resonances and the line widths of all resonances are narrower than those observed for DH-II. In the spectra recorded at 60°C, the two samples are almost identical at the end of the dehydration, and also identical to a spectrum of MH. The change in hydration state from DH to MH is also reflected by a change in chemical shift of around +1 ppm for the carboxylate carbon (Fig. 7a). The effect of heating, with prolonged standing at each heating step, is displayed for DH-I and DH-II in Fig. 7c–f. During dehydration of DH-I, the diagnostic shift is seen for the resonance of the carboxylate carbon, but there are no significant changes observed for the aromatic carbons. This indicates that the arrangement of the aromatic part of the naproxen molecules in DH-I must resemble closely that in MH. On dehydration of DH-II, however, significant changes of the aromatic carbons are observed, in particular for sites C5 and C6. Despite the different dehydration pathways, however, both DH-I and DH-II result finally in the same MH upon heating. Further dehydration to AH is not seen in the NMR experiments because of the sealed sample environment inside the NMR rotor.

DISCUSSION

Summary of the Transformation Pathways

During the DVS analysis (Fig. 2), AH transforms directly to DH-II at 25°C without any intermediate MH formation,

but transforms sequentially to MH then to DH-I at 50°C. This suggests that transformation of AH→DH-II requires minimal activation energy, while AH→MH requires greater activation energy which is supplied only at 50°C. At 25°C, DH-II can proceed to form TH, but this does not happen at 50°C. The absence of TH at 50°C may be attributed to a more rapid rate for TH dehydration at this temperature than for hydration of DH to TH. Moreover, only DH-I is observed at 50°C during both the sorption cycles, which is more stable towards transformation to TH.

Figure 8 summarises the experimentally observed hydration and dehydration pathways for sodium naproxen. As shown in Fig. 8a, under static conditions in desiccators, all of the hydrate forms can be generated within 1 week using the identified optimal conditions, and they remain stable if maintained in the same conditions for at least 3 months. MH and DH-I can be generated by exposing AH at 50°C/50% RH and 50°C/80% RH, respectively. These routes to yield MH and DH-I are different from previously identified methods involving solution crystallisation (DH-I/MH) or dehydration (MH) (20,21,30). The key step is the initial formation of MH from AH, requiring the higher temperature to overcome the apparent activation barrier. Subsequent transformation of MH gives DH-I. DH-I can also be generated at 25°C by exposure of MH at 55% RH in a desiccator. DH-II can only be generated from AH at 25°C/55% RH.

Stability of the DH polymorphs towards interconversion was tested by storage of a bulk sample of DH-I (generated at 50°C/80% RH) at 25°C/55% RH for 2 months. After this time, there was no apparent transformation to DH-II. By contrast, DH-II generated at 25°C/55% RH transforms to DH-I on storage at 50°C/80% RH for 1 week. Thus, DH-I appears to be the more stable dihydrate form. The DH-I sample generated in this manner shows relatively broad XRPD peaks, which may indicate some degree of structural disorder (Supplementary Fig. S4), and it also shows a greater tendency to transform to TH compared to DH-I generated directly from MH at 25°C/55% RH or from AH at 50°C/80% RH. Moreover, if DH-II is kept at 25°C/30% RH for around 2 h to generate MH impurities, the resulting mixture of DH-II and MH generates DH-I over *ca* 1 week at 25°C/55% RH. All of these observations confirm the stability of DH-I over DH-II.

As shown in Fig. 8b, dehydration of TH at 25°C regenerates DH. Both *in-situ* XRPD of TH placed under vacuum at 25°C and bulk samples measured after standing under ambient conditions or in desiccators at 50% RH show mixtures of DH-I and DH-II. Considering the solid-state ^{13}C CP/MAS NMR results (Fig. 7), the transformation of DH-II to MH proceeds with some significant structural rearrangement of the aromatic parts of the naproxen molecules, which is consistent with the rather gradual change observed for DH-II to MH in the DVS desorption cycles at 25°C as compared to the abrupt transformation from DH-I to MH at 50°C (Fig. 2). Moreover, the dehydration pathway under vacuum at low temperature is DH-II→AH and DH-I→MH→AH; while under ambient pressure, the pathway is, DH-II→MH+AH and DH-I→MH. This again confirms the tendency for DH-I to transform to MH; while DH-II transforms directly to AH. At ambient pressure, AH can be generated by dehydration of MH if some activation energy is provided by heating to 60°C.

Influence of Dihydrate Polymorphism on the Transformation Pathways

The DVS data at 25°C show that the distinct behaviour of the dihydrate polymorphs plays a key role in controlling the transformation pathways. The distinct behaviour of the first sorption cycle compared to subsequent sorption cycles is governed by three factors: (i) DH-II is formed directly from AH on increasing the humidity; (ii) DH-I is formed from MH on increasing the humidity; (iii) both DH-I and DH-II transform to the same MH on decreasing the humidity. On account of these properties, the first sorption/desorption cycles in the DVS serve essentially to eliminate AH from the system so that DH-II cannot be formed during any subsequent sorption cycle. The formation of DH-II in the first sorption cycle gives the DVS trace a distinct shape that is not seen in the subsequent cycles. At 50°C, the first sorption cycle also serves to eliminate AH from the system,

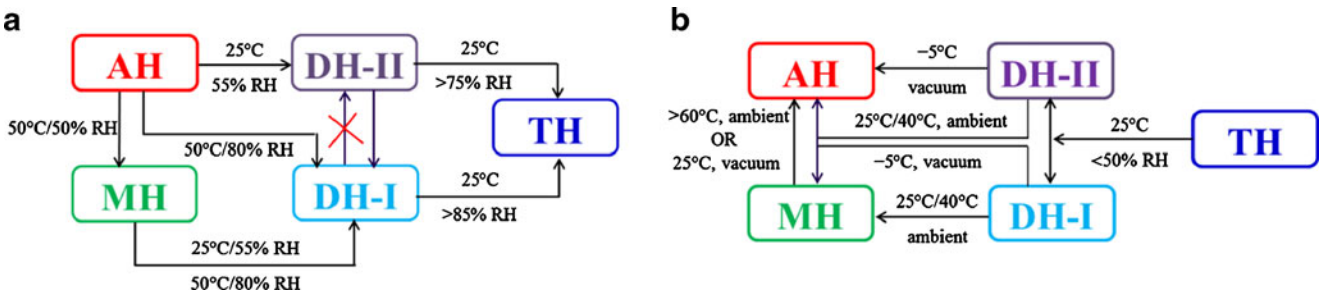

Fig. 8 Experimentally observed transformation pathways among sodium naproxen anhydrate/hydrate forms: (**a**) hydration and (**b**) dehydration.

but the direct formation of MH from AH at this temperature moves the system immediately into the consistent sorption/desorption cycle that is observed subsequently. At 25°C, the critical humidity required for transformation to TH is also significantly different (75% RH for DH-II and 85% RH for DH-I) in the first and second sorption cycles, on account of the different transformation tendencies of DH-II and DH-I.

CONCLUSIONS

The present study shows how carefully programmed DVS analysis can help to explain transformation pathways as a function of temperature and humidity for complex systems where multiple hydrate forms exist. This approach can also help to identify optimal conditions to generate bulk phases by using the presented 3-D empirically-derived phase diagram of the multi-temperature data. In the specific case of sodium (*S*)-naproxen, the nature of the transformation pathways and the results from ^{13}C CP/MAS NMR spectroscopy suggest that the degree of structural rearrangement associated with the various transformations plays an important role in establishing the behaviour of the system.

ACKNOWLEDGMENTS AND DISCLOSURES

We thank the Danish Natural Sciences Research Council for provision of the X-ray equipment at University of Southern Denmark, Odense. The Lundbeck Foundation (grant numbers 479/06 and R31-A2630) and Department of Pharmacy, University of Copenhagen are also acknowledged for financial support. Support from the Danish Council for Independent Research (Technology and Production Sciences, Project number: 09–066411) is also acknowledged. AstraZeneca (Lund, Sweden) is acknowledged for donation of the DVS instrument.

REFERENCES

1. Debnath S, Suryanarayanan R. Influence of processing-induced phase transformations on the dissolution of theophylline tablets. AAPS PharmSciTech. 2004;5(1):E8. Epub 2004/06/17.
2. Khankari RK, Grant DJW. Pharmaceutical hydrates. Thermochim Acta. 1995;248:61–79.
3. Malaj L, Censi R, Gashi Z, Di Martino P. Compression behaviour of anhydrous and hydrate forms of sodium naproxen. Int J Pharm. 2010;390(2):142–9.
4. Phadnis NV, Suryanarayanan R. Polymorphism in anhydrous theophylline—implications on the dissolution rate of theophylline tablets. J Pharm Sci. 1997;86(11):1256–63.
5. Zhang GGZ, Law D, Schmitt EA, Qiu Y. Phase transformation considerations during process development and manufacture of solid oral dosage forms. Adv Drug Delivery Rev. 2004;56(3):371–90.
6. Reutzel-Edens SM, Bush JK, Magee PA, Stephenson GA, Byrn SR. Anhydrates and hydrates of olanzapine: crystallization, solid-state characterization, and structural relationships. Cryst Growth Des. 2003;3(6):897–907.
7. Dong Z, Padden BE, Salsbury JS, Munson EJ, Schroeder SA, Prakash I, *et al.* Neotame anhydrate polymorphs I: preparation and characterization. Pharm Res. 2002;19(3):330–6.
8. Tian F, Rantanen J. Perspective on water of crystallization affecting the functionality of pharmaceuticals. Food Biophys. 2011;6(2):250–8.
9. Van Tonder EC, Maleka TSP, Liebenberg W, Song M, Wurster DE, de Villiers MM. Preparation and physicochemical properties of niclosamide anhydrate and two monohydrates. Int J Pharm. 2004;269(2):417–32.
10. Griesser UJ, Burger A. The effect of water vapor pressure on desolvation kinetics of caffeine 4/5-hydrate. Int J Pharm. 1995;120(1):83–93.
11. Chen LR, Young Jr VG, Lechuga-Ballesteros D, Grant DJW. Solid-state behavior of cromolyn sodium hydrates. J Pharm Sci. 1999;88(11):1191–200.
12. Gillon AL, Davey RJ, Storey R, Feeder N, Nichols G, Dent G, *et al.* Solid state dehydration processes: mechanism of water loss from crystalline inosine dihydrate. J Phys Chem B. 2005;109(11):5341–7.
13. Tian F, Qu H, Louhi-Kultanen M, Rantanen J. Mechanistic insight into the evaporative crystallization of two polymorphs of nitrofurantoin monohydrate. J Cryst Growth. 2009;311(8):2580–9.
14. Brittain HG. Polymorphism and solvatomorphism 2010. J Pharm Sci. 2012;101(2):464–84.
15. Braun DE, Tocher DA, Price SL, Griesser UJ. The complexity of hydration of phloroglucinol: a comprehensive structural and thermodynamic characterization. J Phys Chem B. 2012;116(13):3961–72.
16. Wikström H, Rantanen J, Gift AD, Taylor LS. Toward an understanding of the factors influencing anhydrate-to-hydrate transformation kinetics in aqueous environments. Cryst Growth Des. 2008;8(8):2684–93.
17. Varughese S, Desiraju GR. Using water as a design element in crystal engineering. Host−guest compounds of hydrated 3,5-dihydroxybenzoic acid. Cryst Growth Des. 2010;10(9):4184–96.
18. Clarke HD, Arora KK, Wojtas Ł, Zaworotko MJ. Polymorphism in multiple component crystals: Forms III and IV of gallic acid monohydrate. Cryst Growth Des. 2011;11(4):964–6.
19. Di Martino P, Barthélémy C, Palmieri GF, Martelli S. Physical characterization of naproxen sodium hydrate and anhydrate forms. Eur J Pharm Sci. 2001;14(4):293–300.
20. Kim Y-S, Rousseau RW. Characterization and solid-state transformations of the pseudopolymorphic forms of sodium naproxen. Cryst Growth Des. 2004;4(6):1211–6.
21. Malaj L, Censi R, Martino PD. Mechanisms for dehydration of three sodium naproxen hydrates. Cryst Growth Des. 2009;9(5):2128–36.
22. Martino PD, Barthélémy C, Joiris E, Capsoni D, Masic A, Massarotti V, *et al.* A new tetrahydrated form of sodium naproxen. J Pharm Sci. 2007;96(1):156–67.
23. Feth MP, Nagel N, Baumgartner B, Bröckelmann M, Rigal D, Otto B, *et al.* Challenges in the development of hydrate phases as active pharmaceutical ingredients – An example. Eur J Pharm Sci. 2011;42(1–2):116–29.
24. Gift AD, Taylor LS. Hyphenation of Raman spectroscopy with gravimetric analysis to interrogate water–solid interactions in pharmaceutical systems. J Pharm Biomed Anal. 2007;43(1):14–23.
25. Lane RA, Buckton G. The novel combination of dynamic vapour sorption gravimetric analysis and near infra-red spectroscopy as a hyphenated technique. Int J Pharm. 2000;207(1–2):49–56.
26. Feth MP, Jurascheck J, Spitzenberg M, Dillenz J, Bertele G, Stark H. New technology for the investigation of water vapor sorption–induced crystallographic form transformations of chemical

compounds: a water vapor sorption gravimetry–dispersive raman spectroscopy coupling. J Pharm Sci. 2011;100(3):1080–92.
27. Bennett AE, Rienstra CM, Auger M, Lakshmi KV, Griffin RG. Heteronuclear decoupling in rotating solids. J Chem Phys. 1995;103(16):6951–8.
28. Peersen OB, Wu XL, Kustanovich I, Smith SO. Variable-amplitude cross-polarization MAS NMR. J Magn Reson, Ser A. 1993;104(3):334–9.
29. Ando S, Kikuchi J, Fujimura Y, Ida Y, Higashi K, Moribe K, *et al.* Physicochemical characterization and structural evaluation of a specific 2:1 cocrystal of naproxen-nicotinamide. J Pharm Sci. 2012;101(9):3214–21.
30. Kim Y-s, Paskow HC, Rousseau RW. Propagation of solid-state transformations by dehydration and stabilization of pseudopolymorphic crystals of sodium naproxen. Cryst Growth Des. 2005;5(4):1623–32.